Fusion Engineering and Design 87 (2012) 1770–1776

Contents lists available at SciVerse ScienceDirect

Fusion Engineering and Design

journal homepage: www.elsevier.com/locate/fusengdes

Recent progress of NSTX lithium program and opportunities for magnetic fusion research

M. Ono[a,*], M.G. Bell[a], R. Kaita[a], H.W. Kugel[a], J.-W. Ahn[b], J.P. Allain[c], D. Battaglia[c], R.E. Bell[a], J.M. Canik[b], S. Ding[d], S. Gerhardt[a], T.K. Gray[b], W. Guttenfelder[a], J. Hosea[a], M.A. Jaworski[a], J. Kallman[a], S. Kaye[a], B.P. LeBlanc[a], R. Maingi[b], D.K. Mansfield[a], A. McLean[b], J. Menard[a], D. Muller[a], B. Nelson[e], R. Nygren[f], S. Paul[a], R. Raman[e], Y. Ren[a], P. Ryan[b], S. Sabbagh[g], F. Scotti[a], C. Skinner[a], V. Soukhanovskii[h], V. Surla[i], C.N. Taylor[c], J. Timberlake[a], H.Y. Yuh[j], L.E. Zakharov[a], the NSTX Research Team

[a] *Princeton Plasma Physics Laboratory, PO Box 451, Princeton, NJ 08543, USA*
[b] *Oak Ridge National Laboratory, PO Box 2008, Oak Ridge, TN 37831, USA*
[c] *Purdue University, West Lafayette, IN 47907, USA*
[d] *Academy of Science Institute of Plasma Physics, Hefei, China*
[e] *University of Washington at Seattle, Seattle, WA 98195, USA*
[f] *Sandia National Laboratory, Albuquerque, NM 87185, USA*
[g] *Columbia University, New York, NY 10027, USA*
[h] *Lawrence Livermore National Laboratory, Livermore, CA 94551, USA*
[i] *Center for Plasma-Materials Interactions, University of Illinois, Urbana-Champaign, IL, USA*
[j] *Nova Photonics Inc., Princeton, NJ 08540, USA*

ARTICLE INFO

Article history:
Received 17 May 2011
Received in revised form 26 October 2011
Accepted 27 October 2011
Available online 5 December 2011

Keywords:
International lithium symposium
Tokamaks and spherical tokamaks
Lithium
Plasma–wall interactions

ABSTRACT

Lithium wall coating techniques have been experimentally explored on National Spherical Torus Experiment (NSTX) for the last six years. The lithium experimentation on NSTX started with a few milligrams of lithium injected into the plasma as pellets and it has evolved to a dual lithium evaporation system which can evaporate up to ∼160 g of lithium onto the lower divertor plates between re-loadings. The unique feature of the NSTX lithium research program is that it can investigate the effects of lithium coated plasma-facing components in H-mode divertor plasmas. This lithium evaporation system has produced many intriguing and potentially important results. In 2010, the NSTX lithium program has focused on the effects of liquid lithium divertor (LLD) surfaces including the divertor heat load, deuterium pumping, impurity control, electron thermal confinement, H-mode pedestal physics, and enhanced plasma performance. To fill the LLD with lithium, 1300 g of lithium was evaporated into the NSTX vacuum vessel during the 2010 operations. The routine use of lithium in 2010 has significantly improved the plasma shot availability resulting in a record number of plasma shots in any given year. In this paper, as a follow-on paper from the 1st lithium symposium [1], we review the recent progress toward developing fundamental understanding of the NSTX lithium experimental observations as well as the opportunities and associated R&D required for use of lithium in future magnetic fusion facilities including ITER.

1. Introduction

Various lithium wall-coating techniques have been explored on a number of magnetic fusion devices for over two decades [2–6]. In 2005, the lithium experimental research program on National Spherical Torus Experiment (NSTX) started using a few milligrams of lithium injected as pellets into the plasma. Over the intervening years, the techniques for applying lithium have evolved to the present dual lithium-evaporator system [7] which can deposit hundreds of milligrams of lithium onto the lower divertor plates between discharges and ∼160 g of lithium between re-loadings. In 2010, the total amount of lithium evaporated into the NSTX vessel was ∼1300 g, nearly double the amount evaporated in 2009. The reason for the high lithium evaporation in 2010 was to load the porous surface of the liquid lithium divertor (LLD) plates which had been installed prior to the run. The first physics and technical results obtained with the LLD are reported in references [8,9]. A unique feature of the NSTX lithium program is that it studies the effects of

* Corresponding author. Tel.: +1 609 243 2105; fax: +1 609 243 2222.
E-mail address: mono@pppl.gov (M. Ono).

0920-3796/$ – see front matter © 2011 Elsevier B.V. All rights reserved.
doi:10.1016/j.fusengdes.2011.10.011

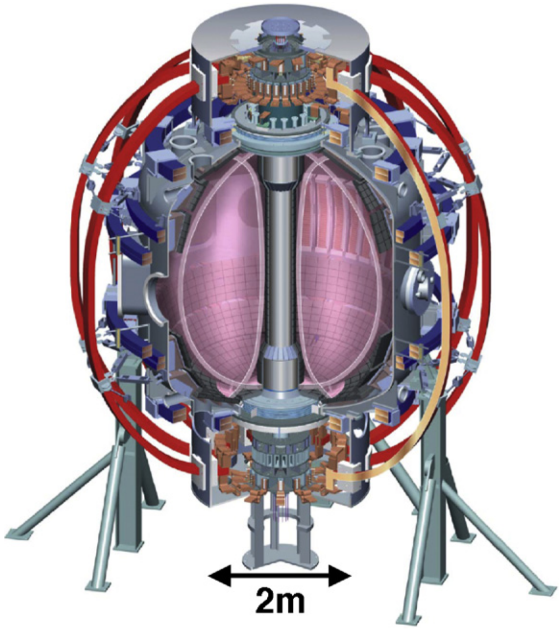

Fig. 1. A schematic of the NSTX device cross section.

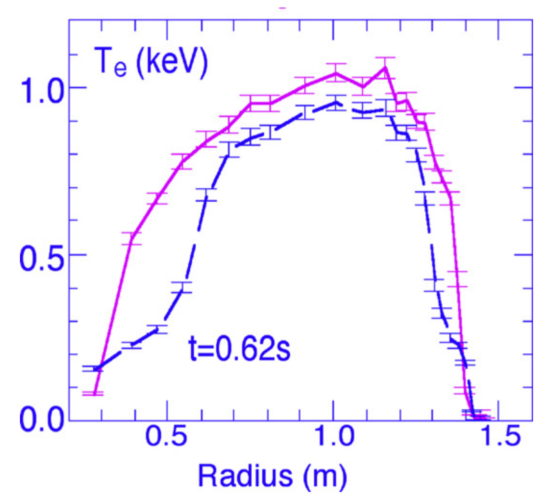

Fig. 2. Profiles of Thomson scattering measurements of electron temperature with (red) and without (blue), lithium close to the time of peak stored energy for, similar H-mode discharges. (For interpretation of the references to color in this figure legend, the reader is referred to the web version of the article.)

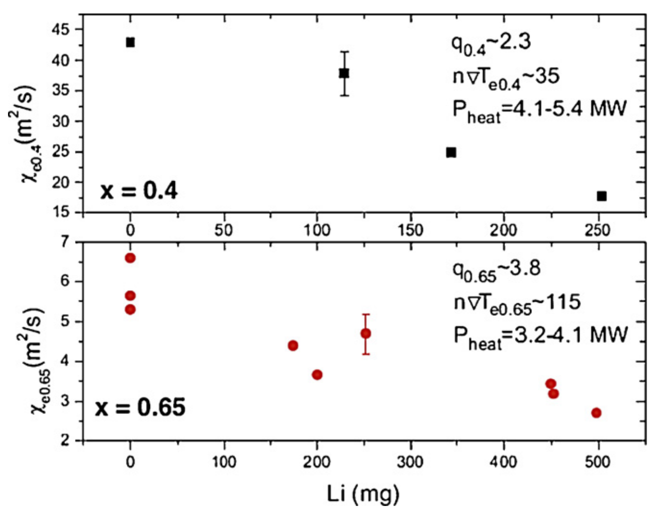

Fig. 3. Electron thermal transport diffusivities from TRANSP analysis in, outer region of the plasma vs. lithium deposited prior to the shot at $x = 0.4$ and 0.65 where x is defined as the square root of the normalized toroidal flux.

solid and liquid lithium divertor surfaces in H-mode divertor plasmas. In the present paper, we will report the recent progress made in the NSTX lithium program in various science areas including electron transport, H-mode power threshold, ELM physics, lithium transport, and liquid lithium surface behavior. We will also point out opportunities and issues that remain to be resolved.

2. Experimental set-up

The National Spherical Torus Experiment (NSTX) is a Mega Ampere (MA)-class Spherical Torus (ST) facility [10] which is designed to explore the low-aspect-ratio tokamak regime to $R/a = 1.35$, as shown in Fig. 1. Presently, the NSTX plasmas are heated by up to 7.5 MW of deuterium Neutral Beam Injection (NBI) and up to 4 MW of High-Harmonic Fast Waves (HHFW) heating and current drive systems. In 2007, a Lithium Evaporator (LITER) was installed on NSTX to explore the effects of lithium coating of its plasma-facing components (PFCs) on the plasma. In 2008, a second LITER was added. The dual LITERs are mounted at the top of the vacuum vessel aiming their lithium vapor streams toward the graphite tiles on the lower divertor. They are separated 150° toroidally to complete the toroidal coverage. Shutters in front of the evaporators prevent lithium entering the plasma region both during the plasma pulse (to prevent lithium deposition on diagnostic windows while their protective shutters are open) and during any subsequent period of He-GDC cleaning (to prevent the entrapment of helium in the deposited lithium layer, though a very minimal amount of He-GDC was performed in 2010). Each LITER system can be removed from the vacuum system through an airlock, refilled with about 80 g of lithium and returned to operation in about two days. In 2010, the LLD system was implemented with an electrical resistive heater system as well as a hot air heater system [8,9]. The LLD surface temperature was monitored by the new dual-band infrared diagnostic system implemented in 2010 [11].

3. Improved electron energy confinement

As previously reported, the lithium evaporation results in broadening of H-mode electron temperature profile compared to plasmas without lithium applied, as shown in Fig. 2 [12,13]. Analysis with the TRANSP code indicates that electron thermal diffusivity in outer region is progressively reduced with increasing lithium evaporation, as shown in Fig. 3 [14]. The improving electron energy confinement with lithium is consistent with the trend of improved confinement with reduced collisionality generally observed in NSTX. Since burning fusion reactor plasmas including ITER rely on heating by fusion alphas, which predominantly heat electrons, the understanding and eventual control of the electron energy transport is of critical importance for magnetic fusion reactor optimization. The ability of lithium application to affect electron transport offers the possibility of testing competing theoretical models, which may lead to resolution of the long standing puzzle of electron energy transport. For example, although Electron Temperature Gradient (ETGs) modes had been observed to play a role in electron energy transport under certain conditions in NSTX, e.g., reversed shear and density gradient ETG stabilizations [15,16], a recent study of the collisionality dependence of the ETG activity in NSTX did not support the view that the ETG is always dominant [17]. However, another electron energy transport model based on

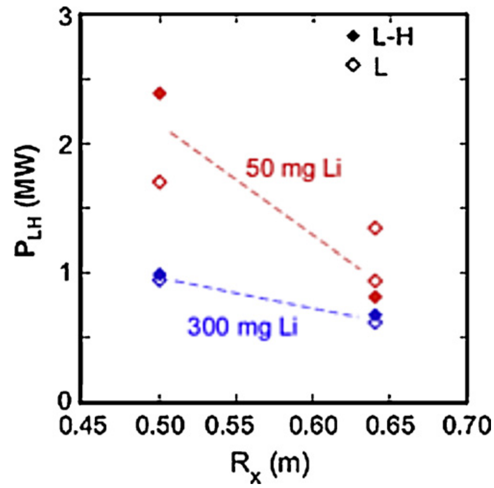

Fig. 4. PLH vs. *x*-point major radius position. P_{LH} is reduced ~35% when lithium deposition increased from 50 to 300 mg.

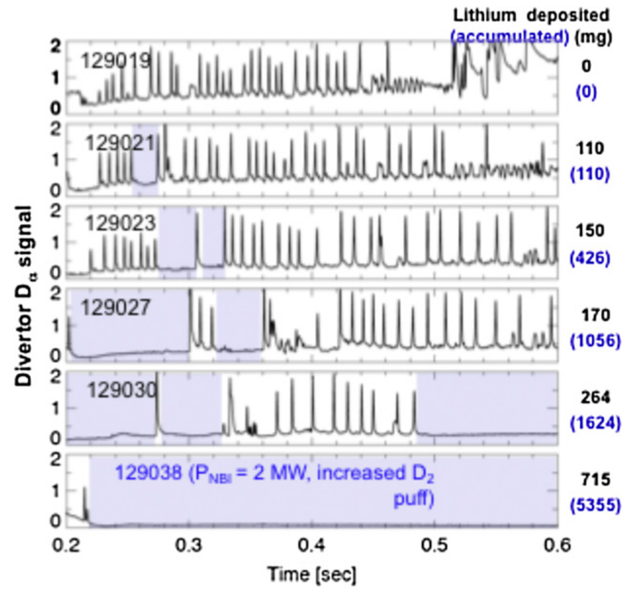

Fig. 5. Temporal edge D-alpha signal for various lithium deposition rate. The regularly occurring spikes represents the Edge Localized Modes (ELMs).

micro-tearing instabilities has been proposed which could explain the observed collisionality dependence of electron transport.

4. H-mode power threshold

The H-mode is desirable for high performance tokamak and ST reactors due to its high confinement and good MHD stability property at high beta [1]. For ITER, predictive modeling shows that fusion Q scales roughly with square of the pedestal pressure so that to fulfill its mission of high fusion gain ($Q = 10$), it is essential to achieve an H-mode with sufficiently high pedestal pressure. In NSTX, a very high confinement regime called the enhanced pedestal H-mode with confinement enhanced relative to the predictions of the ITER 1997 H-mode scaling up to $H_{H98y,2} \sim 1.7$ has been observed following lithium application [18]. This level of confinement is sufficient for future ST devices such as a Fusion Nuclear Science Facility (FNSF) [19] or an ST Pilot Plant [20].

The physics of the H-mode transition is not yet fully understood, so predictions for the heating power required to induce the H-mode (the L–H transition power threshold) in ITER and future ST reactors remains uncertain. On NSTX, the L–H power threshold (P_{LH}) is reduced by up to 40% by applying lithium [21], as seen in Fig. 4. The edge electron confinement improvement with reduced density and edge recycling is likely to be aiding the H-mode transition by increasing the electron temperature near the edge [22]. NSTX research is now focused on understanding the underlying mechanism for the H-mode power threshold reduction which could eventually lead to a fundamental understanding of the H-mode transition itself.

5. H-mode pedestal and ELMs

The edge localized modes (ELMs) are periodic macroscopic instabilities in the H-mode barrier region which can regulate the H-mode barrier (and the associated pressure gradient) and help facilitate steady-state H-mode operation by removing impurities which otherwise accumulate within the barrier. However, ELMs can also cause high transient heat fluxes (typically an order of magnitude higher than the steady-state value) that could render radiative divertor heat load mitigation schemes (such as impurity seeding and detachment) ineffective, leading to damage of the divertor plasma-facing components of future reactors including ITER. In NSTX, the application of lithium can lead to complete suppression of ELMS in H-mode discharges [13], as seen in Fig. 5. While ELM physics is a complex 3D MHD phenomenon, the so-called "peeling-ballooning" model which has been used to model ELMs in other devices has had success in modeling the ELM stabilization following lithium application in NSTX [23]. Detailed profile measurements coupled with analysis of the edge MHD stability show that ELMs become stabilized by the combination of an inward shift of the peak pressure gradient into a region of reduced magnetic shear and a somewhat wider pressure gradient width mainly due to the edge density reduction by lithium. Interpretive analysis [24] of the edge profiles was done with the b2/EIRENE code package. This analysis showed that the magnitude of the edge recycling source was reduced by at least 50%, and that the effective particle and electron thermal diffusion rate from about 2 cm < r-rsep < 5 cm was reduced substantially. Here rsep is the radial location of the separatrix. The magnitude of this reduction increased with the amount of lithium deposited before the discharge. In the region from r-rsep < 2 cm, the edge transport was unchanged or slightly increased. In particular, the electron temperature gradient was invariant, suggesting critical gradient physics. Both paleocalssical transport [25] and electron temperature gradient modes [26] are being investigated as the cause for the underlying transport. The absence of ELMs has also improved particle confinement but this has led to an accumulation in the core of higher Z (predominantly carbon) impurities, and an eventual radiative collapse for some discharges. To control impurities in ELM-free regimes is an active research topic on NSTX. NSTX is working on two impurity reduction strategies. One is to reduce the carbon influx (source). A reduction of carbon impurity level (and Z-effective) was observed when the strike point was placed on LLD instead of carbon tiles [9]. Based on this positive result, NSTX is therefore replacing the inboard graphite divertor tiles with molybdenum-tiles to expand the divertor molybdenum surfaces. NSTX is also trying to reduce carbon accumulation by inducing small ELMs to reduce the particle confinement without significantly reducing the energy confinement. The ELMs were successfully excited with the periodic application of 3D fields which indeed reduced the carbon accumulation without significant energy confinement reduction [27]. NSTX is also planning to install lithium granular injector to induce small ELMs by a periodic injection of lithium granulars into the plasma. The ability of lithium to influence the plasma edge pressure profile and ELMs could also make it a valuable tool for future tokamak experiments including ITER.

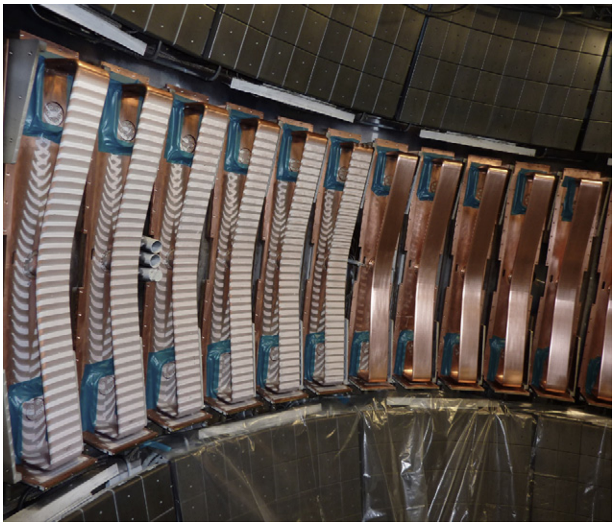

Fig. 6. HHFW antenna straps with Faraday shields remove after the 2010 operations. The left hand side is before cleaning and the right hand side is after cleaning.

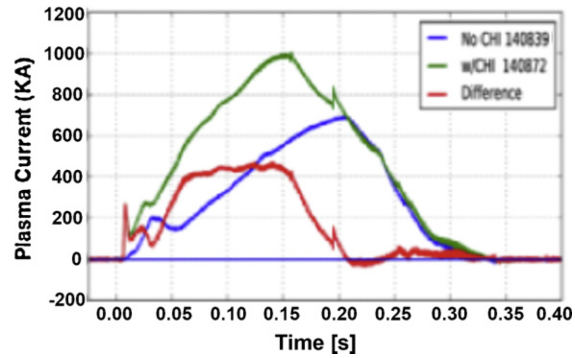

Fig. 7. The green trace is a discharge started with CHI (at 6 ms) and coupled to induction reaching 1 MA at 150 ms. The comparison discharge (blue trace) using the same loop voltage programming, without CHI start-up reaches only 600 kA at the same time. The red trace shows the current difference between the two discharges. (For interpretation of the references to color in this figure legend, the reader is referred to the web version of the article.)

6. High harmonic fast wave heating

In Ref. [1], we noted that the ability of lithium to reduce the edge recycling and the scrape-off-layer density was beneficial for the High-Harmonic Fast Wave (HHFW) heating efficiency [28]. However, in the 2010 campaign, while the HHFW experiments have produced new physics results such as an effective electron heating in a deuterium H-mode at low plasma current for the plasma current ramp-up study, the HHFW antenna power handling capability was significantly degraded. During the rf power pulse, a fast camera viewing the antenna showed signs of arcing apparently triggered by lithium particulates on the antenna Faraday shield surfaces [29]. The arcing spots occurred at sites of heavy lithium accumulation typically located at the top or the bottom areas of the antenna. Also, at the end of the 2010 run, a larger amount of lithium-containing dust was found on the antenna straps and in the bottom of antenna boxes than in prior years. This may have been the result of a number of argon vents of the vacuum system (introducing some level of air contaminations) performed during 2010 after the introduction of lithium. A picture of the HHFW antenna after the 2010 operation is shown in Fig. 6; the left half has not yet been cleaned while the right half has already been cleaned. In the future, we plan to start HHFW operation early in the run to condition antenna to high operating power level prior to heavy lithium application. It should be also noted that the lithium application in NSTX (as previously reported) also greatly enhanced the coupling of electron Bernstein wave (EBW) in H-mode by significantly reducing the edge collisional absorption through reduced edge density and increased edge temperature [30].

7. Improving plasma start-up with coaxial helicity injection

Non-inductive start-up is critically needed for a FNSF due to the limited space for neutron shielding around a central solenoid. To develop a satisfactory solenoid-free start-up technique, NSTX is pursuing a plasma start-up concept using coaxial helicity injection (CHI). The CHI system produces an arc discharge between the inboard and outboard divertor plates which are electrically isolated from each other. In the presence of a toroidal magnetic field, a toroidal current is generated which is amplified by as much as ∼100 compared to the arc current. NSTX has generated toroidal plasma current of up to 300 kA by CHI [31]. After the applied CHI electrode voltage is turned off, the toroidal plasma current ring is pinched off from the injection region forming closed flux surfaces which then decay resistively. At this point, one can apply an toroidal voltage by solenoid induction to further ramp up the current. Since CHI is a DC electrical discharge between electrodes of several kAs, it is most important to control impurity generation. With the application of lithium coating to the electrode region in 2009, it was possible to significantly reduce the influx of impurities (such as oxygen) and produce high quality CHI start-up tokamak discharges which contributed an additional 200 kA to the inductively generated current [32]. In 2010, the CHI performance was further improved through a variety of impurity suppression techniques including absorber arc prevention as well as lithium conditioning. As shown in Fig. 7, the CHI aided start-up produced a significant saving of inductive flux (as much as a factor 50%) to achieve 1 MA discharges with low inductance and low impuritiy levels [31]. For further improvements, the plan is to investigate the effect of a metal electrode (molybdenum tiles on the inboard divertor which acts as the cathode during CHI) to further reduce impurity generation and increase the CHI driven current toward 0.5 MA.

8. Divertor power handling

Handling the steady-state heat flux from fusion plasmas at the divertor surfaces is a challenging technical issue for magnetic fusion reactors. In a tokamak or an ST reactor, the divertor plate can experience a time-averaged peak heat flux of 10–50 MW/m^2, and even higher during transient events such as ELMs and disruptions, so innovative solutions to the plasma material interface are required. While experiments in NSTX were able to demonstrate a significant peak power flux reduction (5–10) by a combination of boundary shaping and divertor gas injection, further peak heat flux reduction would likely to be needed for a steady-state reactor. In 2010, with three divertor PF coils, a stable “snow-flake” divertor configuration was maintained for nearly the entire flat top duration in NSTX. This led to significantly higher expansion of the poloidal flux lines in the divertor, thereby reducing the divertor peak heat flux [33]. The snow-flake divertor with much expanded divertor foot print is very much compatible with the large area diveror pumping surfaces provided by the lithium divertor coating.

In 2010, a Liquid Lithium Divertor (LLD) mounted in the outer divertor was tested with more than enough lithium applied to the LLD surfaces to fill its porous molybdenum surface [8]. A number of interesting observations were made with LLD in use, such as the ability to run a large number of plasma shots (∼ 100 as compared to 2–3 previosuly) without the need to replenish the lithium by evaporation between shots. Even with the heavy lithium deposition onto

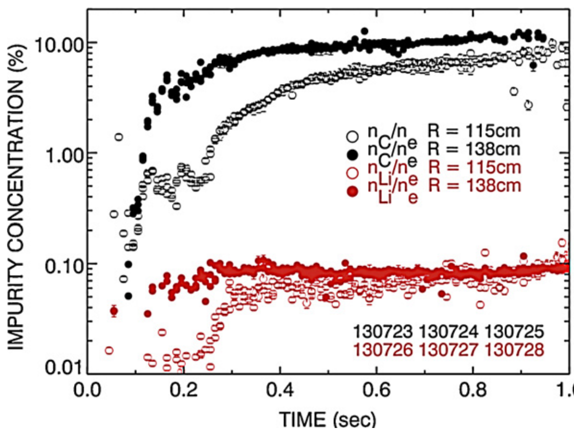

Fig. 8. Temporal evolutions of the lithium (red) and carbon (black) concentration for sets of similar NBI-heated, H-mode discharges for two radial locations as labeled. (For interpretation of the references to color in this figure legend, the reader is referred to the web version of the article.)

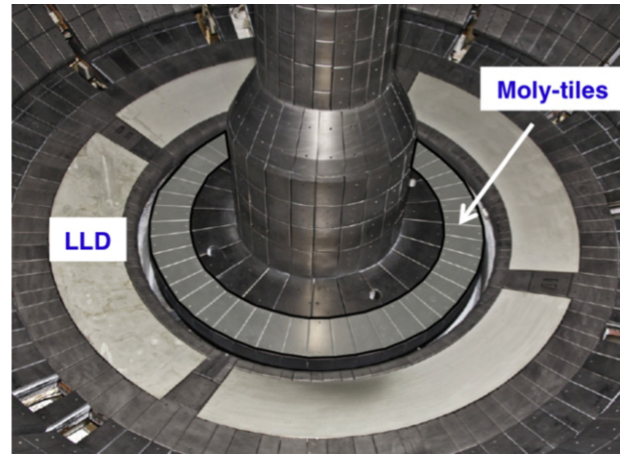

Fig. 10. The 2011 NSTX outboard LLD (with semi-porous molybdenum surface) and inboard molybdenum tile divertor configuration. These surfaces will be coated with lithium by evaporation.

the LLD and the lower divertor area in 2010, the lithium core concentration remained small, as shown in Fig. 8. The results with the LLD confirm that molybdenum could be a good substrate material for liquid or solid lithium surfaces. Even with the divertor strike point directly on the LLD plates, there was no significant molybdenum influx observed. During 2010, extensive measurements of the divertor heat flux were performed, as shown in Fig. 9 [34]. One intriguing result with lithium is a considerable narrowing of the radial width of the heat flux profile projected to the outboard mid-plane of the plasma column, possibly due to the lower edge collisionality and turbulence reduction by lithium.

As discussed in Sec. 5, one row of the graphite tiles on the inboard divertor are being replaced by molybdenum tiles to provide additional molybdenum surfaces, as shown in Fig. 10. One motivation for the increased molybdenum divertor surface coverage is to minimize the carbon influx which can accumulate in the plasma core during extended ELM-free discharges. After the 2011 operation, the NSTX facility plans to undertake a major upgrade where a new center-stack and a second, more tangential NBI system will be installed. This upgrade will essentially double the toroidal magnetic field, plasma current, and heating power. The plasma duration will significantly increase from ∼1 s to ∼5 s [35]. This will present a highly challenging divertor environment in terms of heat flux and pulse duration. The present LLD plates need to be replaced due to the much larger (∼×4) electromagnetic forces expected during disruptions. As one possibility for a post-upgrade divertor configuration, a separate lithium-coated divertor chamber appears to be attractive since the lithium could be largely contained within it. One possible implementation is shown schematically in Fig. 11. Assuming favorable results from analyses and laboratory testing, the molybdenum-tile coverage could be further expanded to the outer divertor region, as the tiles around the entrance to a pumped divertor chamber. A tray containing liquid lithium placed within the divertor chamber could be protected from the plasma as its edges could be hidden behind these tiles. A liquid lithium fill system could also be implemented in the protected area as illustrated in figure. The recessed liquid lithium tray maybe also better protected against electro-magnetic forces such as disruptions. This closed divertor concept may be an important step to test the viability of closed liquid lithium divertor approaches such as an evaporative divertor chamber system [36].

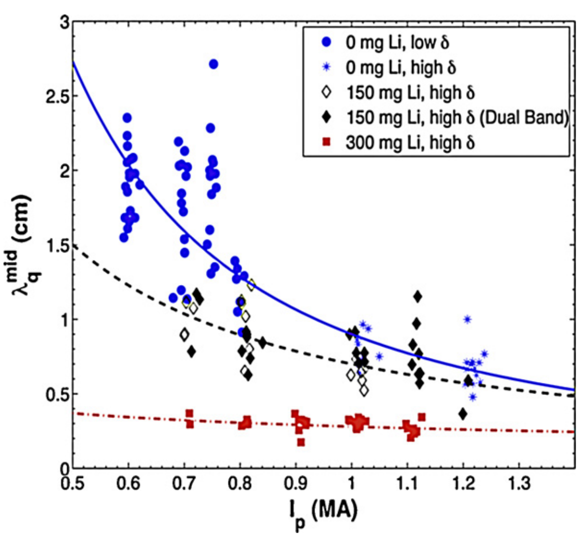

Fig. 9. The outboard divertor heat flux width projected to the outer mid-plane for various level of lithium application as a function of plasma current.

9. Improved plasmas operations

The introduction of lithium evaporators on NSTX has produced a significant benefit to the NSTX plasma operations. The lithium evaporation not only maintains a lower oxygen impurity level but it also controls the level of hydrogenic recycling to

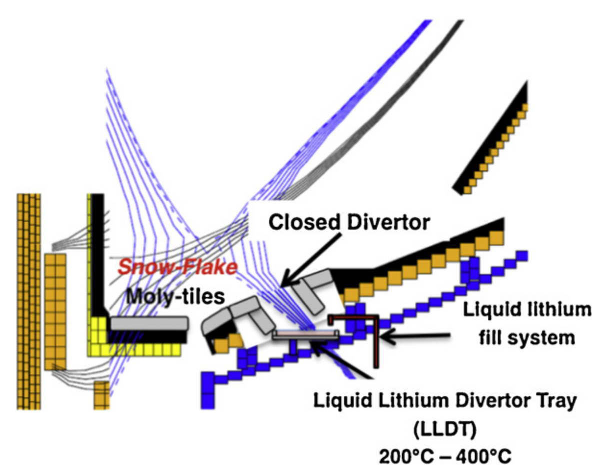

Fig. 11. A possible closed divertor configuration for a post-upgrade NSTX liquid lithium divertor tray.

Table 1
NSTX plasma operations statistics for 2004–2010. The lithium evaporator was used after 2007 and its utilization reached nearly 100% in 2010.

Year	Weeks	Shots	Shots/week	Lithium%
2010	15.4	2941	191	~100
2009	16.8	2750	163	92
2000	16.5	2570	156	46
2007	12.6	1890	150	69
2006	12.7	1615	127	0
2005	18.0	2221	124	0
2004	21.1	2460	117	0

enable reproducible plasma shots without the time consuming between-shots helium glow-discharge cleaning. The lithium application also tends to produce more quiescent plasmas for ELMs and rotating, lower frequency MHD modes which further improves the operational reliability. The precise mechanism of MHD activity reduction with lithium is still not well understood though the progress has been made for example for the lithium ELM stabilization as mentioned in Section 5. As can be seen in Table 1, the NSTX operational efficiency indicated by the number of successful plasma shots per one run-week has steadily improved since the introduction of lithium evaporators in 2007. Since the NSTX experimental proposals are formulated based on the number of plasma shots, the larger number of plasma shots directly contributes toward the scientific productivity of the facility. In 2010, almost all experimental operation was conducted with lithium applied which contributed to the record number of 191 shots per week compared to the previous record of 163 shots per week in 2009, as well as the total of 2941 shots obtained in one year compared to the previous record of 2750 in 2009. The operation with lithium improved the number of plasma shots per week by about 50% over the pre-lithium period before 2007 as shown in Table 1. In addition to the lithium application, there were improvements due to the operational experience. This can be seen in the improving trend shown in table during year 2004–2006 (without lithium) and after 2007 as the plasma operation is getting used to handling lithium. By 2010, the shot # per week has approached the maximum operational limit of ~200 with lithium.

The effectiveness of lithium compared to the boronization previously used in NSTX may be attributable to the fact that the lithium is applied between shots whereas the boronization is applied only periodically, every several hundred plasma shots, so the benefit of boronization becomes degraded over time. One noteworthy advantage of lithium, which is not well understood, is its effectiveness in producing a rapid recovery from venting the vacuum vessel. The NSTX plasma start-up after extended opening to air requires a bake-out of its carbon tiles at 350 °C, which usually takes about 3 weeks to remove water absorbed within the carbon tiles. With boronization, it usually takes several more weeks of operation to reach a long-pulse H-mode, which is an indicator of a good plasma operating condition. With the introduction of lithium, the time can be reduced to a few days following the bakeout. During 2010, because of the heavy lithium evaporation, there were a number of argon vents to replace and repair lithium evaporator shutters and gate valves. By applying lithium immediately, satisfactory plasma operation could be obtained practically immediately after an argon vent, although the reasons for this are not clear. The lithium application does not appear to directly correlate with the partial pressure of residual impurity gases such as O, O_2, CO, CO_2, etc. There is also no obvious correlation with the level of O impurity line emission, the H/D ratio, etc. The highly effective lithium application for the quick vent recovery indicates that the tokamak start-up process is a complex process which would merit a further investigation.

The post-operation lithium clean-up process performed during the maintenance period is described in the companion paper by Kugel et al. [9].

10. Conclusions and discussions

The evaporation of lithium onto the lower divertor region in NSTX has yielded a number of important benefits in terms of intriguing science results and operational improvements. The improved electron confinement in the outer region increased the overall plasma performance. The lower recycling and the changes in the pedestal region produced by lithium also reduced the H-mode power threshold and affected the ELMs, including producing their complete suppression. The lithium dropper which can inject lithium powder during the plasma discharge was developed on NSTX [37]. This type of real time lithium injection maybe attractive for future long pulse reactors such as ITER. In 2010, the NSTX dropper has been successfully applied on the long-pulse super conducting EAST tokamak plasma for improved H-mode access and attainment of long-pulse discharges [38]. The ability of lithium to reduce edge density and impurity levels improved the HHFW (ICRF) core heating efficiency and non-inductive start-up by CHI. However, in 2010, the HHFW operation encountered a problem with arcing due to lithium-related deposits on the antenna, likely to have been produced by inadvertent air contamination during the argon vents performed during the run.

In 2010, the use of liquid lithium on the divertor surfaces was investigated for the first time. The liquid lithium appears to be resilient as a divertor surface with no significant impurity influx, even when the outer divertor strike point, which takes the majority of the divertor power flux, is located on it. This bodes well for future liquid lithium divertor development. Operationally, the lithium conditioning has improved the NSTX plasma performance in terms of more reliable plasma operations with about 50% increase in the number of plasma shots achieved per week compared to the pre-lithium operation periods. While there are still many remaining questions, the understanding of lithium–plasma interactions is rapidly growing. Overall, lithium as a PFC material has a very exciting prospect in contributing to magnetic fusion research as a tool to control the plasma edge and as a potential solution for the very challenging magnetic fusion reactor divertor heat flux problem.

Acknowledgement

This work was supported by DoE Contract No. DE-AC02-09CH11466.

References

[1] M. Ono, M.G. Bell, R.E. Bell, R. Kaita, H.W. Kugel, et al., Fusion Eng. Des. 85 (2010) 882.
[2] D.K Mansfield, D.W. Johnson, B. Grek, H.W. Kugel, M.G. Bell, R.E. Bell, et al., Nucl. Fusion 41 (2001) 1823.
[3] S.V. Mirnov, V.B. Lazarev, S.M. Sotnikov, T-11M Team, V.A. Evtikhin, I.E. Lyublinski, A.V. Verkov, Fusion Eng. Des. 65 (2003) 455–465.
[4] M.L. Apicella, et al., J. Nucl. Mater. 363–365 (1346–51) (2007).
[5] J. Sanchez, F.L. Tabares, D. Tafalla, J.A. Ferreira, I. Garcia-Cortes, C. Hidalgo, et al., J. Nucl. Mater. 390–391 (852–7) (2009).
[6] R. Majeski, R. Doerner, T. Gray, R. Kaita, R. Maingi, D. Mansfield, et al., Phys. Rev. Lett. 97 (2006) 075002.
[7] H.W. Kugel, M.G. Bell, H. Scheneider, J.P. Allain, et al., Fusion Eng. Des. 85 (2010) 865.
[8] H.W. Kugel, D. Mansfield, A.L. Roquemore, et al., IAEA Fusion Energy Conference FTP/3-6Ra, 2010.
[9] H.W. Kugel, et al., Fusion Eng. Des. (2011), doi:10.1016/j.fusengdes.2011.07.010.
[10] M. Ono, S.M. Kaye, Y.-K.M. Peng, G. Barnes, et al., Nucl. Fusion 40 (2000) 557.
[11] A.G. McLean, J.-W. Ahn, T.K. Gray, R. Maingi, et al., 2nd ISLA, 2011.
[12] H.W. Kugel, M.G. Bell, J.-W. Ahn, J.P. Allain, et al., Phys. Plasmas 15 (2008) 056118.
[13] M.G. Bell, et al., Plasma Phys. Controlled Fusion 51 (2009) 124056.

[14] S. Ding, et al., PPCF 52 (2010) 015001.
[15] H.Y. Yuh, S.M. Kaye., F.M. Levinton, E. Mazzucato, et al., Phys. Rev. Lett. 106 (2011) 055003.
[16] Y. Ren, S.M. Kaye, E. Mazzucato, W. Guttenfelder, et al., Phys. Rev. Lett. 106 (2011) 165005.
[17] W. Guttenfelder, J. Candy, S.M. Kaye, et al., Phys. Rev. Lett. 106 (2011) 155004.
[18] R. Maingi, R.E. Bell, J.M. Canik, et al., Phys. Rev. Lett. 105 (2010) 135004.
[19] Y-K.M. Peng, T.W. Burgess, A.J. Carroll, et al., Fusion Sci. Technol. 56 (2009) 957.
[20] J.E. Menard, L. Bromberg, T. Brown, et al., Nucl. Fusion 51 (10) (2011) 103014.
[21] S.M. Kaye, R. Maingi, D. Battaglia, et al., IAEA Fusion Energy Conference EXC/2-3Rb, 2010.
[22] D. Battaglia, C.S. Change, S.M. Kaye, et al., Bull. Am. Phys. Soc. 56 (2011) 248.
[23] R. Maingi, T.H. Osborne, B.P. LeBlanc, R.E. Bell, et al., Phys. Rev. Lett. 103 (2009) 075001.
[24] J.M. Canik, R. Maingi, S. Kubota, et al., Physic of Plasmas 18 (2011) 056118.
[25] J.D. Callen, R.J. Groebner, T.H. Osborne, et al., Nucl. Fusion 50 (2010) 064004.
[26] A.M. Dimits, G. Bateman, M.A. Beer, et al., Phys. Plasmas 7 (2000) 969.
[27] J.M. Canik, R. Maingi, T.E. Evanc, R.E. Bell, S.P. Gerhardt, B.P. LeBlanc, et al., Phys. Rev. Lett. 104 (045001) (2010).
[28] J. Hosea, R.E. Bell, B.P. LeBlanc, C.K. Phillips, et al., Phys. Plasmas 15 (2008) 056104.
[29] P.M. Ryan, et al., US-Japan RF Plasma Physics Workshop, Toba, Japan, 8–9 February, 2011.
[30] S.J. Diem, G. Taylor, J.B. Caughman, P.C. Efthimion, H. Kugel, B.P. LeBlanc, et al., Nucl. Fusion 49 (2009) 095027.
[31] B.A. Nelson, T.R. Jarboe, D. Mueller, R. Raman, et al., Nucl. Fusion 51 (2011) 063008.
[32] R. Raman, D. Mueller, B.A. Nelson, T.R. Jarboe, et al., Phys. Rev. Lett. 104 (2010) 095003.
[33] V.A. Soukhanovskii1, J.-W. Ahn, R.E. Bell, et al., Nucl. Fusion 51 (2011) 012001.
[34] T.K. Gray, R. Maingi, A.G. McLean, et al., IAEA Fusion Energy Conference EXD/P3-13, 2010.
[35] J. Menard, J. Canik, B. Covele, et al., 3th EPS Conference of Plasma Physics, P2.106, 2010.
[36] Y. Nagayama, Fusion Eng. Des. 84 (2009) 1380.
[37] D.K. Mansfield, A.L. Roquemore, H. Schneider, et al., Fusion Eng. Des. 85 (2010) 890.
[38] G.S. Xu, B.N. Wan, J.G. Li, et al., Nucl. Fusion 51 (2011) 072001.